Published in final edited form as:
Neuroscience. 2006 December 28; 143(4): 1051–1064.

STEREOLOGICAL ESTIMATES OF THE BASAL FOREBRAIN CELL POPULATION IN THE RAT, INCLUDING NEURONS CONTAINING CHOLINE ACETYLTRANSFERASE (ChAT), GLUTAMIC ACID DECARBOXYLASE (GAD) OR PHOSPHATE-ACTIVATED GLUTAMINASE (PAG) AND COLOCALIZING VESICULAR GLUTAMATE TRANSPORTERS (VGluTs)

I. GRITTI[a], **P. HENNY**[b], **F. GALLONI**[a], **L. MAINVILLE**[b], **M. MARIOTTI**[a], and **B. E. JONES**[b,*]

a *Dipartimento di Scienze Cliniche Luigi Sacco, Università degli Studi di Milano, Via Giovan Battista Grassi 74, Milan, Italy 20157*

b *Department of Neurology and Neurosurgery, McGill University, Montreal Neurological Institute, 3801 University Street, Montreal, Quebec, Canada H3A 2B4*

Abstract

The basal forebrain (BF) plays an important role in modulating cortical activity and influencing attention, learning and memory. These activities are fulfilled importantly yet not entirely by cholinergic neurons. Noncholinergic neurons also contribute and are comprised by GABAergic neurons and other possibly glutamatergic neurons. The aim of the present study was to estimate the total number of cells in the BF of the rat and the proportions of that total represented by cholinergic, GABAergic and glutamatergic neurons. For this purpose, cells were counted using unbiased stereological methods within the medial septum, diagonal band, magnocellular preoptic nucleus, substantia innominata and globus pallidus in sections stained for Nissl substance and/or the neurotransmitter enzymes, choline acetyltransferase (ChAT), glutamic acid decarboxylase (GAD) or phosphate-activated glutaminase (PAG). In Nissl-stained sections, the total number of neurons in the BF was estimated as ~355,000 and the numbers of ChAT-immuno-positive (+) as ~22,000, GAD + ~119,000 and PAG+ ~316,000, corresponding to ~5%, ~35% and ~90% of the total. Thus, of the large population of BF neurons, only a small proportion has the capacity to synthesize acetylcholine (ACh), one third to synthesize GABA and the vast majority to synthesize glutamate (Glu). Moreover, through the presence of PAG, a proportion of ACh- and GABA-synthesizing neurons also have the capacity to synthesize Glu. In sections dual fluorescent immunostained for vesicular transporters, VGluT3 and not VGluT2 was present in the cell bodies of most PAG+ and ChAT+ and half the GAD + cells. Given previous results showing that VGluT2 and not VGluT3 was present in BF axon terminals and not colocalized with VAChT or VGAT, we conclude that the BF cell population influences cortical and subcortical regions through neurons which release ACh, GABA or Glu from their terminals but which in part can also synthesize and release Glu from their soma or dendrites.

*Correspondence author: Tel: 514-398-1913; Fax: 514-398-5871 E-mail address: barbara.jones@mcgill.ca.

Section editor: Charles R. Gerfen

Keywords

acetylcholine; GABA; glutamate; diagonal band; medial septum; magnocellular preoptic nucleus; substantia innominata; globus pallidus

As evident from the devastating effects of lesions, the basal forebrain (BF) plays a critical role in cortical and state modulation, which influences sleep-wake states, attention, learning and memory (Damasio et al., 1985; Dunnett et al., 1991; Wenk, 1997; Sarter et al., 2003; Jones, 2004). This role has been attributed particularly to the cholinergic neurons and their widespread projections to the allo- and neo-cortex. Yet, selective neurotoxic lesions of the cholinergic neurons have not produced the same overwhelming effects as the total lesions of the BF (Lee et al., 1994; Baxter et al., 1995; Gerashchenko et al., 2001), indicating that other BF neurons participate in cortical and state modulation. It is thus important to characterize and quantify the noncholinergic as well as cholinergic constituents of the BF cell population.

Acetylcholine (ACh)-synthesizing neurons are distributed across BF nuclei of the medial septum-diagonal band of Broca (MS-DBB), from where they give rise to prominent projections to hippocampus, and the magnocellular preoptic-substantia innominata-globus pallidus (MCPO-SI-GP), from where they give rise to prominent projections to neocortex (Rye et al., 1984). Another well defined contingent of the BF cell population contains the synthetic enzyme for GABA. Neurons containing glutamic acid decarboxylase (GAD) are codistributed with the those containing choline acetyltransferase (ChAT), and large GAD-positive (+) neurons project in parallel with ChAT+ neurons from the MS-DBB to the allocortex and from the MCPO-SI-GP to the neocortex (Kohler et al., 1984; Brashear et al., 1986; Zaborszky et al., 1986; Fisher et al., 1988; Freund and Antal, 1988; Freund and Meskenaite, 1992; Gritti et al., 1993; Gritti et al., 1997). In contrast to ChAT+ neurons, GAD+ neurons also give rise to important descending projections to the hypothalamus and brainstem (Semba et al., 1989; Gritti et al., 1994), and they likely also include local interneurons. In the BF, the GAD+ plus the ChAT+ neurons do not account for all the cortically projecting, nor for all the caudally projecting BF neurons (Gritti et al., 1997; Gritti et al., 2003). It was thus proposed that the nonGABAergic, noncholinergic BF neurons are likely glutamatergic neurons.

The synthesis of glutamate (Glu) as a neurotransmitter in neurons occurs from the substrate glutamine, which is taken up from glia, and by the mitochondrial enzyme phosphate-activated glutaminase (PAG) (Bradford et al., 1978). In immunohistochemical studies in the neocortex, PAG was found to be contained predominantly in pyramidal neurons and rarely in GABAergic interneurons (Donoghue et al., 1985; Kaneko and Mizuno, 1988; Akiyama et al., 1990; Kaneko et al., 1992; Kaneko and Mizuno, 1994; Van der Gucht et al., 2003). In a previous study, we thus utilized PAG to label Glu-synthesizing neurons in the BF (Manns et al., 2001). In that study, we found that a major proportion of neocortically projecting BF neurons contained PAG and would accordingly have the capacity to synthesize Glu as a neurotransmitter. By applying stereology, we sought in the present study to determine the total numbers of ChAT+, GAD+ and PAG+ neurons along with the total number of all, Nissl-stained, neurons in the BF of the rat.

Given that the numbers and proportions of PAG+ cells exceeded that of the ChAT-negative (−) and GAD- cells in the present study and that a proportion of ChAT+ and GAD+ cells were found to be PAG+ in a previous study (Manns et al., 2001), we also examined in the present study whether ChAT+, GAD+ and/or PAG+ cells contained the vesicular transporters for Glu (VGluT) and could thus store and release Glu as a neurotransmitter (Fremeau et al., 2001; Fujiyama et al., 2001; Fremeau et al., 2002). Using RT-PCR or in situ for mRNA or immunohistochemistry for protein, VGluT2 has been found to be synthesized in BF neurons

and transported along their axons to terminals from where it is released as a neurotransmitter and VGluT3 to be contained in BF nerve cell bodies and dendrites from where it can be released to act as a retrograde signal (Harkany et al., 2003; Hajszan et al., 2004; Colom et al., 2005; Danik et al., 2005; Hur and Zaborszky, 2005; Henny and Jones, 2006). Employing colchicine treatment to block axonal transport, we examined dual immunostaining by fluorescence for the enzymes and VGluTs to determine the proportion of each cell type that would have the capacity to release Glu.

EXPERIMENTAL PROCEDURES

Animals and surgery

Results from six adult male Wistar rats (Charles River Canada, St. Constant, Quebec, Canada), weighing approximately 250 grams, are reported in this study. All procedures were approved by the McGill University Animal Care Committee and conform to standards of the Canadian Council on Animal Care. For surgery or euthanasia, the rats were anesthetized with sodium pentobarbital (Somnotol, 65 mg/kg, i.p.). Three rats were operated ~24 hours prior to killing for injections of colchicine (50 μg in 25 μl saline) into the lateral ventricle, as previously applied (Gritti et al., 1993; Gritti et al., 1997) for enhancing levels of GAD in cell bodies and here for also enhancing levels of VGluTs within dual-immunostained tissue (below). All rats were killed by perfusion with a fixative through the ascending aorta.

Perfusion and fixation

Brains were fixed with Zamboni's solution, according to a slight modification of the procedure developed by Kaneko for immunostaining of the PAG enzyme (Kaneko and Mizuno, 1988; Kaneko et al., 1989; Manns et al., 2001). Following a brief rinse with phosphate buffered saline, the animals were perfused through the ascending aorta with 500 ml of a modified Zamboni's solution of 0.3% paraformaldehyde and 75% saturated picric acid in 0.1 M sodium phosphate buffer (pH 7.0, over ~30 minutes). The brains were post-fixed overnight at 4°C in a solution of 3% paraformaldehyde with 75% saturated picric acid (pH 7.0). They were subsequently immersed in a solution of 30% sucrose at 4°C for ~72 hours for cryoprotection. Brains were then frozen at −50°C and stored at −80°C.

Immunohistochemistry

Coronal sections were cut on a freezing microtome with a thickness of 20 μm, which was established as the thickest that allowed full and even penetration of antibodies (particularly for PAG). The sections were collected at 400 μm intervals in twenty adjacent series used for different immunostaining. For random starting and ordering of the series, a random number generator was employed to determine which series would be immunostained with ChAT, GAD or PAG in each brain. The sections were collected in phosphate buffer (pH 7.4; 0.1M).

For peroxidase immunostained series (from 3 untreated rats, G1, G2 and G3), sections were first incubated in a Tris-saline solution (TS, 0.1 M) containing bovine serum albumin (BSA) at 3% for prior blocking and at 1% for all other applications. As previously employed (Gritti et al., 2003), antisera for ChAT (from rabbit, 1:2000) were obtained from Chemicon International (Temecula, CA, USA: AB143). Also previously employed (Manns et al., 2001), antisera for PAG (from rabbit, 1:6000) were kindly supplied by Dr. T. Kaneko (Kyoto, Japan) who originally showed that the antisera recognizes two bands of peptides at 62 and 65 kD, corresponding to the two isoforms of rat brain PAG (Akiyama et al., 1990). Also previously employed (Gritti et al., 2003), antisera for GAD (from rabbit, 1:3000) were obtained from Chemicon (AB108) and shown by them using Western Blot to recognize a 67 kD band of protein from rat brain, corresponding to GAD67. Sections were incubated overnight at room temperature with primary antibodies for ChAT and PAG or for three nights at 4^{o} C with those

for GAD. The sections were subsequently incubated with donkey anti-rabbit antiserum (1:100, Jackson ImmunoResearch Laboratories, West Grove, PA, USA) followed by rabbit peroxidase-antiperoxidase (PAP, 1:200, Jackson). PAP was revealed using diaminobenzidine (DAB) in the presence of 0.1% glucose oxidase in Tris-buffer (pH 7.4) during 15 min for ChAT, 13 min for PAG and 17 min for GAD. For the PAG series, DAB was intensified with nickel (DAB-Ni), and the sections were counterstained for Nissl using Neutral Red (NR).

For dual fluorescent immunostained series (from 3 colchicine treated rats, G5, G6 and G7), sections were incubated in a Tris-saline solution (0.1 M) containing Triton x-100 at 0.1% and normal donkey serum (NDS) at 3% for prior blocking and at 1% for the rest of the procedure. The primary antibodies for VGluT2 and VGluT3 (both from guinea pig) were obtained from Chemicon (AB5907 and AB5421, respectively) and were found in previous studies (Henny and Jones, 2006) to provide staining similar to that published with other antibodies for these proteins (Fremeau et al., 2001; Fremeau et al., 2002). The primary antibody for GAD (from mouse) was obtained from Chemicon (MAB5406) and shown by them to recognize a 67 kD band in rat brain. Sections were co-incubated overnight at room temperature with the primary antibodies against 1) VGluT2 (1:5000) and PAG (as above), 2) VGluT3 (1:1000) and PAG (as above), 3) VGluT3 and ChAT (as above), or 4) VGluT3 and GAD67 (1:500). The sections were then co-incubated for 2 hours with Cy3-conjugated donkey anti-guinea pig (1:1000, Jackson, for VGluT2 or VGluT3) and Cy2-conjugated donkey anti-rabbit (1:200, Jackson, for ChAT or PAG) or Cy2-conjugated donkey anti-mouse (1:200, Jackson, for GAD67).

Controls were routinely carried out by replacing the primary antisera with normal sera from the same species and at the same concentration to insure that nonspecific staining did not occur. After processing, all sections were washed in phosphate buffer, mounted out of TS, dehydrated through graded alcohols, delipidated in xylene and coverslipped using Permount (Fisher, Fair Lawn, NJ, USA).

Stereological analysis

Sections were viewed using a Leica DMLB microscope equipped with an x/y/z movement-sensitive stage and video camera connected to a computer. Cells were plotted and images acquired for figures using Neurolucida software (MicroBrightField, MBF, Williston, VT, USA). In three brains processed for peroxidase immunostaining, cells were counted using StereoInvestigator software (MBF). Plotting and counting were done using a computer resident atlas of the forebrain, which was designed according to cytoarchitectonic and chemoarchitectonic principles (Geeraedts et al., 1990; Gritti et al., 1993). For this purpose, outlines of sections and contours of the major nuclei were drawn in Neurolucida from series of sections which were collected at 400 μm intervals üver-Berrera, ChAT and GAD. The levelsstained of the atlas correspond approximately to those of the Paxinos and Watson atlas (Paxinos and Watson, 1986), although from anterior (A) 8.6 (from interaural zero), at which level our sections are matched to the Paxinos and Watson atlas, extending rostrally and caudally, they differ slightly (~10% difference). For stereological estimates, cell counts were performed within the atlas contours of the BF nuclei in 12 plotting and illustrating the distribution of cells in the BF nuclei, cells were plotted in 6 sections at 800 μm intervals. In each case, atlas templates using low magnification (5 or 10x) objectives. When necessary the contours of the atlas were slightly adjusted to fit the nuclei of the histology section. Plotting or counting was then performed within the contours at high magnification using a 63x Oil objective with a 1.4 numerical aperture and an oil condenser. For plotting cells for illustration of their distribution in figures using Neurolucida, all labeled neuronal cell profiles in the BF nuclei contours were marked through the full depth of individual(20 μm thick cut) sections.

In each series of three brains (G1, G2 and G3) immunostained by peroxidase, immuno-positive (+) or NR+ cells were counted by applying systematic unbiased sampling using the Optical

Fractionator probe of StereoInvestigator. The cells were counted within 6 nuclei in the BF: MS, DBB, MCPO, SIa, SIp and GP. For each nucleus, labeled cells were counted on one side of the brain in at least 4 sections (4 – 7, depending upon the length of each nucleus) at 400 μm intervals (1/20 sections sampled). A counting frame of 89 x 89 μm (7921μm^2) and a sampling grid of μm 200 ^{2}) were employed. Since the average thickness of x 200 μm (40,000 the mounted sections was ~10 μm across series surface was employed. From the top surface of each section, cells were counted if the top of the cell came into focus beneath the surface and within the dissector height. The sampling thus included 5% of the sections, ~20% of the area of each nucleus and ~80% of the height of the section for an overall sampling of ~0.8% of the volume of each nucleus through the BF. Accordingly, an average of ~894 sampling sites were employed for counting cells in an average total volume for the six BF nuclei of ~11.34 mm^3. In initial sampling and for the duration of the counting, the precision of the estimates was checked by referring to Gundersen's Coefficient of Error (CE, m1). The average CE (in 3 brains) for the total number of cells across the BF was 0.08 for the ChAT+ cells, 0.04 for the GAD+ cells, 0.02 for the PAG+/NR+ cells and 0.06 for the PAG−/NR+ cells.

Additional series processed for dual fluorescent immunostaining for VGluTs and PAG, ChAT, or GAD were analyzed under epifluorescent microscopy on the Leica DMLB microscope equipped with filters appropriate for Cy2 (FITC) and Cy3 (rhodamine) detection. In each dual immunostained series of three brains (G5, G6 and G7), immuno-positive cells were counted by applying systematic unbiased sampling using the Optical Fractionator probe of StereoInvestigator for estimates of proportions of double-labeled cells within the MCPO at one level (~A8.2). The probe was run twice in each series, so as to sample the same population of cells but with different (Cy3 or Cy2) filters. A counting frame of 89 x 89 μm (7921 μm^2) and a sampling grid of μm 200 ^{2}) were employed, such as to sample an average ofx 200 μm (40,000 ~30 sites in each series. A dissector height of 8 μm was used in this series of mounted sections which had an average thickness of 8 μm.

Color photographs were prepared using Adobe Photoshop and schematic figures from the computer atlas images from Neurolucida using Adobe Illustrator (Adobe Systems, San Jose, CA, USA).

RESULTS

Distribution and estimates of ChAT+, GAD+ and PAG+ neurons

As evident in the MCPO (Fig. 1), ChAT+, GAD+ and PAG+ neurons were codistributed through the nuclei of the BF cholinergic cell area. Darkly stained with DAB, ChAT+ cells were most commonly medium to large in size, fusiform to polygonal in shape and in some regions grouped in clusters (Fig. 1A). Also darkly stained with DAB, GAD+ cells were variable in size from small to large, oval to polygonal in shape and relatively densely distributed through all areas where cholinergic cells were present (Fig. 1B). In some places, large GAD+ cells also formed small aggregates. Stained in a punctate manner with black DAB-Ni, PAG+ neurons were also variable in size from small to large, oval to polygonal in shape and more numerous than the ChAT+ or GAD+ cells (Fig. 1C). PAG+/NR+ cells were codistributed with less numerous NR+ cells that did not contain PAG+ punctate staining and were thus considered PAG−/NR+ cells. Like the PAG+/NR+, these were also variable in size and shape. Along with GAD+ cells, the PAG+ cells were evident across all the BF nuclei where cholinergic cells were located, including the MCPO (Fig. 1), the DBB (Fig. 2A), the SIa (Fig. 2B), the SIp (Fig. 2C) and the GP (Fig. 2D). In each of these areas, the PAG+/NR+ cells were codistributed with less numerous PAG−/NR+ cells (Fig. 2). All cell types were also present in the olfactory tubercle (OTu), but were not included in the present survey.

From rostral to caudal, ChAT+ cells were distributed through the MS, DBB, MCPO, SIa, SIp and GP (Fig. 3), in some places in aggregates, as described previously (Gritti et al., 1993). Ubiquitously, though not evenly, intermingled with the ChAT+ cells, GAD+ cells were densely distributed through the same regions (Fig. 4). Throughout, PAG+/NR+ cells were present in the highest density along with less numerous PAG−/NR+ (Fig. 5).

Using the Optical Fractionator probe of StereoInvestigator, total cell numbers were estimated for each cell type across the BF nuclei from three rats (G1, G2 and G3; Table 1). The average total numbers of cells estimated in this manner were ~22,000 ChAT+ cells, ~119,000 GAD+ cells, ~315,000 PAG+ cells and 350,000 (PAG+/and PAG−/) NR+ cells. According to these estimates the cell densities were ~2000 ChAT+, 11,000 GAD+ cells, 28,000 PAG+ and 31,000 NR+ cells per mm^3. The relative proportions of cells were ~5% ChAT+, 35% GAD+ and 90% PAG+ of the total (NR+) cell population. Except within the GP, these proportions were similar across nuclei of the BF.

Proportions of PAG+, ChAT+ and GAD+ neurons containing VGluT

In order to determine if PAG+, ChAT+ and/or GAD+ cells contained VGluTs, dual fluorescent immunostained series were examined from colchicine treated rats (G5, G6 and G7). In series dual immunostained for PAG and VGluT2 (Fig. 6A), the VGluT2 staining was prominent within axon terminals and varicosities (Fig. 6A2). In contrast, it was not evident at levels above background in cell bodies of neurons in the BF, despite colchicine pretreatment. Under these conditions, PAG+ nerve cell bodies were judged to be negative for VGluT2 immunostaining (Fig. 6A1 and A2).

In series dual immunostained for the synthetic enzymes and VGluT3 (Fig. 6B-D), the VGluT3 staining was prominent in a small number of axon terminals and in many nerve cell bodies. In sections dual immunostained for PAG and VGluT3, most PAG+ cells contained VGluT3 (Fig. 6B1 and B2). Using unbiased estimates through the MCPO, approximately 70% of PAG+ cells were judged to be immuno-positive for VGluT3 (mean ± standard deviation from three rats, SD: 70.3% ± 26.7%). Reciprocally, almost all VGluT3+ neurons were positively stained for PAG (96.3% ± 4.4%). In sections dual immunostained for ChAT and VGluT3, the vast majority of ChAT+ neurons were judged immuno-positive for VGluT3 (Fig. 6C1 and C2). Indeed, VGluT3 was present in ~90% of the ChAT+ cells (88.9% ± 19.2%). In sections dual immunostained for GAD and VGluT3, about half of the GAD+ neurons were judged to be immuno-positive for VGluT3 (46.8% ± 21.6%) (Fig. 6D1 and D2).

DISCUSSION

The present stereological estimates reveal a very large cell population in the BF of the rat that is comprised of only a small proportion of ACh-synthesizing neurons together with a significant proportion of GABA-synthesizing neurons and major proportion of Glu-synthesizing neurons. Given the overlapping numbers, a proportion of ACh- and GABA-synthesizing neurons could also synthesize Glu. The vast proportion of Glu-synthesizing neurons also appear to have the capacity to store and release Glu either through VGluT2, which is present in axon terminals, or through VGluT3, which is present in most Glu- and ACh- and about half the GABA-synthesizing nerve cell bodies. These results indicate that glutamate can be synthesized in the cell bodies of a major proportion of BF cells and if not released from terminals, released from the soma or dendrites of glutamatergic but also many cholinergic and GABAergic neurons to contribute to the local processing as well as efferent output and consequential functional influence of the BF.

Numbers and proportions of neurons able to synthesize ACh, GABA and/or Glu

We employed stereological analysis for estimating total cell numbers through the volume of the BF nuclei in the present study. We first had to determine appropriate immunohistochemical processing and stereological procedures for counting immunostained cells. We learned that we could not use sections thicker than 20 μm in order to have full and even penetration of the antibodies for ChAT, GAD and PAG through the full depth of the sections. We subsequently found that these sections were reduced to an average 10 μm thickness once they were dehydrated, delipidated and coverslipped. We were thus not able to apply what are otherwise considered to be optimal conditions for stereological counts which set guard zones at the top and bottom of the sections and count through more than 10 μm through the middle of the section (West, 1993). We adopted a strategy instead of counting the tops of cells which came into focus beneath the surface of the section and through 8 μm of the z axis. We moreover had to count cells based upon their immunostaining and thus of the cytoplasm, not the nucleus, which we thus did for the NR staining of the cytoplasm as well. Given several adjacent series of sections that were stained from each brain, we randomized the start of each series and collected sections at every 400 μm. This collection procedure thus provided for sampling of each series, 12 sections through the BF cholinergic cell area and 4 to 7 sections through each individual nucleus, depending upon its length. We subsequently selected a counting frame size that would provide >3 cells on average to be counted per frame per series across the BF. And finally we selected a grid size that provided >100 cells of each type to be counted per series across the BF. In practice, the sampling proved to be just adequate for the ChAT+ cells and more than adequate for the other cells, particularly the PAG+ cells.

We obtained an average estimate of ChAT+ cells of ~22,000 which is higher than the average estimate, ~15,000 (excluding the OTu), we previously calculated using counts corrected for double counting according to estimates of cell size and section thickness by the Abercrombie method (Abercrombie, 1946). However, these two estimates are not statistically significantly different when compared between the two groups and thus support the contention that Abercrombie corrected counts can be successfully used to estimate cell numbers if applied appropriately (Guillery and Herrup, 1997). In the present sample, the variation across brains was relatively high with a coefficient of variation (CV: SD/mean) of 0.33. It is not known if this variation is due to sampling of what is an inhomogeneously distributed population of cells that tend to cluster in groups or to individual variation in the number of cells across rats. To our knowledge, there is one other published estimate of the total number of ChAT+ cells in the rat BF which is 26,390 (Miettinen et al., 2002).

The number of GAD+ cells, ~119,000, estimated here by stereology significantly and greatly exceeds the number, ~30,000 (excluding the OTu), previously estimated by us using Abercrombie corrected counts (Gritti et al., 1993). This three fold difference cannot be attributed to differences in counting method. It is undoubtedly due to the use of a different antibody for staining GAD. In our previous study, we employed the original sheep anti-GAD antiserum (Oertel et al., 1981), whereas in the current study we employed the more recent rabbit anti-GAD antiserum directed against the GAD67 isoform of the enzyme (Chemicon), which is present in the soma of most GABAergic cells and appears to provide greater sensitivity for staining cell bodies at least in the BF. We did also find a relatively large variation in the number of GAD+ cells across brains with a CV of 0.39. As for the ChAT+ cells, it could be due to the somewhat uneven distribution of GAD+ cells. It could also be due to individual differences in numbers of GAD+ cells. Such variation for GAD+ neurons (stained for GAD67) has been noted by others using stereological estimates in the dentate gyrus and associated with a CV of 0.40 (Muller et al., 2001). In those studies, the variation was actually attributed to individual variation in the number of GAD+ cells across rats (see below). For comparison, we know of no other estimates for GAD+ cell numbers across the BF.

The number of PAG+ neurons was estimated here at ~316,000. This estimated number had the smallest CV of 0.14, indicating possibly that the large number and density as well as more even distribution of the PAG+ neurons was associated with more similar estimates across brains. Or it indicates that there is less variation in the number of PAG+ neurons. By adding the number of PAG−/NR+ neurons to those of the PAG+/NR+ neurons, we estimated the total population of cells in the BF as ~355,000 with a CV of 0.15. We know of no other published estimates of PAG+ or total BF cell population.

The PAG+ neurons represented ~90% of the BF cell population. Given that the ChAT+ cells represent ~5% and the GAD+ ~35%, it appears that there is an overlap in the three populations. We first employed PAG based upon immunohistochemical studies showing that it selectively labeled glutamatergic pyramidal cells and rarely labeled GABAergic interneurons in the cortex (Donoghue et al., 1985; Kaneko and Mizuno, 1988; Akiyama et al., 1990; Kaneko et al., 1992; Kaneko and Mizuno, 1994). On the other hand, in our previous study we found that PAG was present in ~95% of ChAT+ cells and ~60% of GAD+ (also >50% of parvalbumin+) cells in the BF (Manns et al., 2001; Gritti et al., 2003). As discussed in that original study on cortically projecting neurons, the colocalization of these neurotransmitter enzymes could indicate that Glu could be synthesized and utilized together with ACh and GABA in the same neurons. PAG can also serve to provide Glu for the synthesis of GABA (Pow and Robinson, 1994). The clear presence of PAG- neurons in the BF, indicates that certain neurons do not contain this enzyme for the conversion of glutamine to Glu. In the cortex, evidence was presented that GABAergic interneurons do not contain PAG and contain instead high concentrations of soluble aspartate aminotransferase (sAAT) through which they could utilize α-ketoglutarate to produce Glu as a precursor for GABA (Kaneko and Mizuno, 1994). The numbers of the PAG−/NR+ cells (~39,000) correspond to approximately 40% of the GAD+ cell population that was the proportion of GAD+ cells found to be negative for PAG in our previous study (Manns et al., 2001). Together with our previous results, the present results suggest that some neurons contain PAG and GAD and have the capacity to synthesize both Glu and GABA or to utilize Glu synthesized by PAG for GABA synthesis, whereas others have the capacity to synthesize GABA alone through a different metabolic pathway for Glu. Perhaps the capacity for some PAG+ neurons to synthesize GABA from Glu through the presence of GAD is realized under certain conditions, as has been found for what are glutamatergic neurons in the dentate gyrus, which in addition to PAG, express GAD, and synthesize and release GABA following kindling (Kaneko and Mizuno, 1988; Sloviter et al., 1996; Gomez-Lira et al., 2005).

Proportions of neurons able to release Glu through VGluTs

Since implementation of immunohistochemical staining of the synthetic enzymes for ACh, GABA and Glu, the vesicular transporter proteins have been identified, which are responsible for the uptake, storage and release of ACh (VAChT) (Gilmor et al., 1996), GABA (VGAT) (Chaudhry et al., 1998) and Glu (VGluT 1 and 2) from nerve terminals (Fremeau et al., 2001; Fujiyama et al., 2001). Presence of specific vesicular transporters in terminals of neurons thus indicates use of the substrate as a neurotransmitter. Whereas VAChT is present in the soma and dendrites of cholinergic neurons, VGAT and VGluT1/2 are only found in the axonal varicosities and terminals. Some investigators have visualized VGluT2 in nerve cell bodies of neurons in the MS-DBB using very high doses (3 times those used in the present study) of colchicine (Hajszan et al., 2004; Colom et al., 2005), yet such doses also stimulate mRNA for many enzymes and peptides (Cortes et al., 1990). Using previously established and approved doses of colchicine which block axonal transport (Gritti et al., 1993), we were unable to detect VGluT2 in nerve cell bodies of neurons in the BF. It was thus not possible to employ immunohistochemical staining of cell bodies for this vesicular transporter to determine which BF neurons utilize Glu. In situ hybridization for mRNA of the vesicular transporters has been successfully employed in BF and revealed that some neurons contain mRNA for VGluT2 (Hur

and Zaborszky, 2005). From RT-PCR studies, it also appeared that mRNA for VGluT2 can be colocalized with mRNA for ChAT and/or GAD in young and adult rats (Sotty et al., 2003; Danik et al., 2005). Thus, as for the presence of PAG, the presence of mRNA for VGluT2 in ChAT and GAD expressing neurons suggested that BF neurons have the potential to synthesize Glu and the vesicular transporters necessary for its utilization along with ACh or GABA as neurotransmitters. In contrast, by immunohistochemical study of the vesicular transporters contained in anterogradely labeled BF terminals, we have found that the BF fibers are phenotypically distinct, containing VAChT, VGAT or VGluT2 in their terminals, and thus functionally cholinergic, GABAergic or glutamatergic (Henny and Jones, 2006). In the descending projections to the hypothalamus, the VAChT+ terminals represented a small proportion (~10%), the VGAT+ terminals the largest proportion (~50%) and the VGluT2+ terminals ~25%. The estimate of glutamatergic BF projection neurons in our studies is similar to that recently estimated for the MS-DBB, though using different techniques, as representing 20–25% (Colom et al., 2005). On the other hand, these similar estimates leave in further question why such a large proportion of BF neurons contain PAG, including ChAT+ and GAD + neurons.

In addition to VGluT1 and 2, a third type of VGluT was discovered and found to be present in cell bodies as well as terminals of neurons and moreover to be present within cholinergic neurons in the striatum (Gras et al., 2002) and GABAergic interneurons in the cortex (Fremeau et al., 2002; Herzog et al., 2004). VGluT3 was also reported to be present in many BF neurons, including both cholinergic and presumed GABAergic, parvalbumin-immunostained, neurons in most BF nuclei (Harkany et al., 2003). In the present study, we confirmed that VGluT3 is present in the soma of BF neurons, and showed that it is present in neurons dual-immunostained for ChAT, GAD or PAG. In our previous studies, we did not find VGluT3 to be contained in terminals of BF projecting fibers to either hypothalamus (Henny and Jones, 2006) or cortex (Henny and Jones, in preparation). Its presence in the cell bodies thus presumably does not indicate that the cells have the capacity to release Glu from axon terminals. On the other hand, VGluT3 has been shown to endow the soma and dendrites of cells with the capacity to release Glu that can act as a retrograde signal upon afferent inputs (Fremeau et al., 2002; Harkany et al., 2003; Harkany et al., 2004). Here, the vast majority of ChAT+ cells and about half the GAD+ cells were judged immuno-positive for VGluT3. These proportions are very similar to those estimated for the ChAT+ and GAD+ cells that respectively contained PAG (Manns et al., 2001), indicating together with our previous results showing a lack of VGluT3 in BF terminals (above, (Henny and Jones, 2006)), that these neurons would have the capacity to synthesize and release Glu not from axon terminals but from their cell bodies or dendrites. A large proportion (~70%) of PAG+ neurons were immunostained for VGluT3 and virtually all VGluT3+ neurons were immunostained for PAG, indicating that most Glu-synthesizing neurons would have the capacity to release Glu from their cell bodies or dendrites. It is thus possible that the presence of PAG in ChAT+ and GAD+ neurons (Manns et al., 2001) does reflect the capacity to synthesize Glu as a neurotransmitter or modulator, however one which is released through VGluT3 from the soma and dendrites of neurons which otherwise release ACh or GABA through VAChT or VGAT respectively from their axon terminals. The presence of PAG in ChAT- and GAD- neurons likely reflects the capacity of those neurons to synthesize Glu as a neurotransmitter that can be released from axon terminals presumably through VGluT2 and/or from cell bodies through VGluT3. Accordingly, the presence of PAG in the major proportion of BF neurons indicates that in addition to ACh and GABA, Glu plays a major part in the distant and local influences of the BF neurons.

Given the large population of BF neurons and the small percentage comprised by the cholinergic cells, it is not surprising that nonselective lesions of the BF have had much more devastating effects upon cortical activity and behavioral state than selective cholinergic cell lesions (Damasio et al., 1985; Dunnett et al., 1991; Wenk, 1997; Sarter et al., 2003; Jones,

2004). Thus the important role played by the cholinergic cells must be viewed as contingent upon the influence of the predominant GABAergic and glutamatergic cells along with the potential modulation exerted by Glu, which can be synthesized and released from such a large proportion of BF neurons.

Acknowledgements

The research was supported by grants to IG and MM from the University of Milan and to BEJ from the Canadian Institutes of Health Research (CIHR, 13458) and the National Institute of Mental Health (NIMH, RO1 MH60119-01A1). We are most grateful to Dr. Takeshi Kaneko (Kyoto, Japan) for generously supplying the antibody for PAG. We would also like to thank Dr. Gianluca Vago (Department of Clinical Science Luigi Sacco, University of Milan, Milan, Italy) for his consultation.

References

Abercrombie M. Estimation of nuclear population from microtome sections. Anat Rec 1946;94:239–247.

Akiyama H, Kaneko T, Mizuno N, McGeer PL. Distribution of phosphate-activated glutaminase in the human cerebral cortex. J Comp Neurol 1990;297:239–252. [PubMed: 2196285]

Baxter MG, Bucci DJ, Gorman LK, Wiley RG, Gallagher M. Selective immunotoxic lesions of basal forebrain cholinergic cells: effects on learning and memory in rats. Behav Neurosci 1995;109:714–722. [PubMed: 7576215]

Bradford HF, Ward HK, Thomas AJ. Glutamine--a major substrate for nerve endings. J Neurochem 1978;30:1453–1459. [PubMed: 670985]

Brashear HR, Zaborszky L, Heimer L. Distribution of GABAergic and cholinergic neurons in the rat diagonal band. Neuroscience 1986;17:439–451. [PubMed: 3517690]

Chaudhry FA, Reimer RJ, Bellocchio EE, Danbolt NC, Osen KK, Edwards RH, Storm-Mathisen J. The vesicular GABA transporter, VGAT, localizes to synaptic vesicles in sets of glycinergic as well as GABAergic neurons. J Neurosci 1998;18:9733–9750. [PubMed: 9822734]

Colom LV, Castaneda MT, Reyna T, Hernandez S, Garrido-Sanabria E. Characterization of medial septal glutamatergic neurons and their projection to the hippocampus. Synapse 2005;58:151–164. [PubMed: 16108008]

Cortes R, Ceccatelli S, Schalling M, Hokfelt T. Differential effects of intracerebroventricular colchicine administration on the expression of mRNAs for neuropeptides and neurotransmitter enzymes, with special emphasis on galanin: an in situ hybridization study. Synapse 1990;6:369–391. [PubMed: 1705058]

Damasio AR, Graff-Radford NR, Eslinger PJ, Damasio H, Kassell N. Amnesia following basal forebrain lesions. Arch Neurol 1985;42:263–271. [PubMed: 3977657]

Danik M, Cassoly E, Manseau F, Sotty F, Mouginot D, Williams S. Frequent coexpression of the vesicular glutamate transporter 1 and 2 genes, as well as coexpression with genes for choline acetyltransferase or glutamic acid decarboxylase in neurons of rat brain. J Neurosci Res 2005;81:506–521. [PubMed: 15983996]

Donoghue JP, Wenthold RJ, Altschuler RA. Localization of glutaminase-like and aspartate aminotransferase-like immunoreactivity in neurons of cerebral neocortex. J Neurosci 1985;5:2597–2608. [PubMed: 4045547]

Dunnett SB, Everitt BJ, Robbins TW. The basal forebrain-cortical cholinergic system: interpreting the functional consequences of excitotoxic lesions. Trends Neurosci 1991;14:494–501. [PubMed: 1726766]

Fisher RS, Buchwald NA, Hull CD, Levine MS. GABAergic basal forebrain neurons project to the neocortex: The localization of glutamic acid decarboxylase and choline acetyltransferase in feline corticopetal neurons. J Comp Neurol 1988;272:489–502. [PubMed: 2843581]

Fremeau RT Jr, Burman J, Qureshi T, Tran CH, Proctor J, Johnson J, Zhang H, Sulzer D, Copenhagen DR, Storm-Mathisen J, Reimer RJ, Chaudhry FA, Edwards RH. The identification of vesicular glutamate transporter 3 suggests novel modes of signaling by glutamate. Proc Natl Acad Sci U S A 2002;99:14488–14493. [PubMed: 12388773]

Fremeau RT Jr, Troyer MD, Pahner I, Nygaard GO, Tran CH, Reimer RJ, Bellocchio EE, Fortin D, Storm-Mathisen J, Edwards RH. The expression of vesicular glutamate transporters defines two classes of excitatory synapse. Neuron 2001;31:247–260. [PubMed: 11502256]

Freund TF, Antal M. GABA-containing neurons in the septum control inhibitory interneurons in the hippocampus. Nature 1988;336:170–173. [PubMed: 3185735]

Freund TF, Meskenaite V. Gamma-aminobutyric acid-containing basal forebrain neurons innervate inhibitory interneurons in the neocortex. Proc Natl Acad Sci USA 1992;89:738–742. [PubMed: 1731348]

Fujiyama F, Furuta T, Kaneko T. Immunocytochemical localization of candidates for vesicular glutamate transporters in the rat cerebral cortex. J Comp Neurol 2001;435:379–387. [PubMed: 11406819]

Geeraedts LMG, Nieuwenhuys R, Veening JG. Medial forebrain bundle of the rat: III. Cytoarchitecture of the rostral (telencephalic) part of the medial forebrain bundle bed nucleus. J Comp Neurol 1990;294:507–536. [PubMed: 2341624]

Gerashchenko D, Salin-Pascual R, Shiromani PJ. Effects of hypocretin-saporin injections into the medial septum on sleep and hippocampal theta. Brain Res 2001;913:106–115. [PubMed: 11532254]

Gilmor ML, Nash NR, Roghani A, Edwards RH, Yi H, Hersch SM, Levey AI. Expression of the putative vesicular acetylcholine transporter in rat brain and localization in cholinergic synaptic vesicles. J Neurosci 1996;16:2179–2190. [PubMed: 8601799]

Gomez-Lira G, Lamas M, Romo-Parra H, Gutierrez R. Programmed and induced phenotype of the hippocampal granule cells. J Neurosci 2005;25:6939–6946. [PubMed: 16049169]

Gras C, Herzog E, Bellenchi GC, Bernard V, Ravassard P, Pohl M, Gasnier B, Giros B, El Mestikawy S. A third vesicular glutamate transporter expressed by cholinergic and serotoninergic neurons. J Neurosci 2002;22:5442–5451. [PubMed: 12097496]

Gritti I, Mainville L, Jones BE. Codistribution of GABA- with acetylcholine-synthesizing neurons in the basal forebrain of the rat. J Comp Neurol 1993;329:438–457. [PubMed: 8454735]

Gritti I, Mainville L, Jones BE. Projections of GABAergic and cholinergic basal forebrain and GABAergic preoptic-anterior hypothalamic neurons to the posterior lateral hypothalamus of the rat. J Comp Neurol 1994;339:251–268. [PubMed: 8300907]

Gritti I, Mainville L, Mancia M, Jones BE. GABAergic and other non-cholinergic basal forebrain neurons project together with cholinergic neurons to meso- and iso-cortex in the rat. J Comp Neurol 1997;383:163–177. [PubMed: 9182846]

Gritti I, Manns ID, Mainville L, Jones BE. Parvalbumin, calbindin, or calretinin in cortically projecting and GABAergic, cholinergic, or glutamatergic basal forebrain neurons of the rat. J Comp Neurol 2003;458:11–31. [PubMed: 12577320]

Guillery RW, Herrup K. Quantification without pontification: choosing a method for counting objects in sectioned tissues. J Comp Neurol 1997;386:2–7. [PubMed: 9303520]

Hajszan T, Alreja M, Leranth C. Intrinsic vesicular glutamate transporter 2-immunoreactive input to septohippocampal parvalbumin-containing neurons: novel glutamatergic local circuit cells. Hippocampus 2004;14:499–509. [PubMed: 15224985]

Harkany T, Hartig W, Berghuis P, Dobszay MB, Zilberter Y, Edwards RH, Mackie K, Ernfors P. Complementary distribution of type 1 cannabinoid receptors and vesicular glutamate transporter 3 in basal forebrain suggests input-specific retrograde signalling by cholinergic neurons. Eur J Neurosci 2003;18:1979–1992. [PubMed: 14622230]

Harkany T, Holmgren C, Hartig W, Qureshi T, Chaudhry FA, Storm-Mathisen J, Dobszay MB, Berghuis P, Schulte G, Sousa KM, Fremeau RT Jr, Edwards RH, Mackie K, Ernfors P, Zilberter Y. Endocannabinoid-independent retrograde signaling at inhibitory synapses in layer 2/3 of neocortex: involvement of vesicular glutamate transporter 3. J Neurosci 2004;24:4978–4988. [PubMed: 15163690]

Henny P, Jones BE. Vesicular glutamate (VGluT), GABA (VGAT), and acetylcholine (VAChT) transporters in basal forebrain axon terminals innervating the lateral hypothalamus. J Comp Neurol 2006;496:453–467. [PubMed: 16572456]

Herzog E, Gilchrist J, Gras C, Muzerelle A, Ravassard P, Giros B, Gaspar P, El Mestikawy S. Localization of VGLUT3, the vesicular glutamate transporter type 3, in the rat brain. Neuroscience 2004;123:983–1002. [PubMed: 14751290]

Hur EE, Zaborszky L. Vglut2 afferents to the medial prefrontal and primary somatosensory cortices: a combined retrograde tracing in situ hybridization. J Comp Neurol 2005;483:351–373. [PubMed: 15682395]

Jones BE. Activity, modulation and role of basal forebrain cholinergic neurons innervating the cerebral cortex. Progr Brain Res 2004;145:157–169.

Kaneko T, Itoh K, Shigemoto R, Mizuno N. Glutaminase-like immunoreactivity in the lower brainstem and cerebellum of the adult rat. Neuroscience 1989;32:79–98. [PubMed: 2586753]

Kaneko T, Mizuno N. Immunohistochemical study of glutaminase-containing neurons in the cerebral cortex and thalamus of the rat. J Comp Neurol 1988;267:590–602. [PubMed: 2450108]

Kaneko T, Mizuno N. Glutamate-synthesizing enzymes in GABAergic neurons of the neocortex: a double immunofluorescence study in the rat. Neuroscience 1994;61:839–849. [PubMed: 7838383]

Kaneko T, Nakaya Y, Mizuno N. Paucity of glutaminase-immunoreactive nonpyramidal neurons in the rat cerebral cortex. J Comp Neurol 1992;322:181–190. [PubMed: 1381731]

Kohler C, Chan-Palay V, Wu J-Y. Septal neurons containing glutamic acid decarboxylase immunoreactivity project to the hippocampal region in the rat brain. Anat Embryol 1984;169:41–44. [PubMed: 6721220]

Lee MG, Chrobak JJ, Sik A, Wiley RG, Buzsaki G. Hippocampal theta activity following selective lesion of the septal cholinergic system. Neuroscience 1994;62:1033–1047. [PubMed: 7845584]

Manns ID, Mainville L, Jones BE. Evidence for glutamate, in addition to acetylcholine and GABA, neurotransmitter synthesis in basal forebrain neurons projecting to the entorhinal cortex. Neuroscience 2001;107:249–263. [PubMed: 11731099]

Miettinen RA, Kalesnykas G, Koivisto EH. Estimation of the total number of cholinergic neurons containing estrogen receptor-alpha in the rat basal forebrain. J Histochem Cytochem 2002;50:891–902. [PubMed: 12070268]

Muller GJ, Moller A, Johansen FF. Stereological cell counts of GABAergic neurons in rat dentate hilus following transient cerebral ischemia. Exp Brain Res 2001;141:380–388. [PubMed: 11715083]

Oertel WH, Schmechel DE, Mugnaini E, Tappaz ML, Kopin IJ. Immunocytochemical localization of glutamate decarboxylase in rat cerebellum with a new antiserum. Neuroscience 1981;6:2715–2735. [PubMed: 7033824]

Paxinos, G.; Watson, C. The Rat Brain in Stereotaxic Coordinates. Academic Press; Sydney: 1986.

Pow DV, Robinson SR. Glutamate in some retinal neurons is derived solely from glia. Neuroscience 1994;60:355–366. [PubMed: 7915410]

Rye DB, Wainer BH, Mesulam M-M, Mufson EJ, Saper CB. Cortical projections arising from the basal forebrain: a study of cholinergic and noncholinergic components employing combined retrograde tracing and immunohistochemical localization of choline acetyltransferase. Neuroscience 1984;13:627–643. [PubMed: 6527769]

Sarter M, Bruno JP, Givens B. Attentional functions of cortical cholinergic inputs: what does it mean for learning and memory? Neurobiol Learn Mem 2003;80:245–256. [PubMed: 14521867]

Semba K, Reiner PB, McGeer EG, Fibiger HC. Brainstem projecting neurons in the rat basal forebrain: neurochemical, topographical, and physiological distinctions from cortically projecting cholinergic neurons. Brain Res Bull 1989;22:501–509. [PubMed: 2469525]

Sloviter RS, Dichter MA, Rachinsky TL, Dean E, Goodman JH, Sollas AL, Martin DL. Basal expression and induction of glutamate decarboxylase and GABA in excitatory granule cells of the rat and monkey hippocampal dentate gyrus. J Comp Neurol 1996;373:593–618. [PubMed: 8889946]

Sotty F, Danik M, Manseau F, Laplante F, Quirion R, Williams S. Distinct electrophysiological properties of glutamatergic, cholinergic and GABAergic rat septohippocampal neurons: novel implications for hippocampal rhythmicity. J Physiol 2003;551:927–943. [PubMed: 12865506]

Van der Gucht E, Jacobs S, Kaneko T, Vandesande F, Arckens L. Distribution and morphological characterization of phosphate-activated glutaminase-immunoreactive neurons in cat visual cortex. Brain Res 2003;988:29–42. [PubMed: 14519524]

Wenk GL. The nucleus basalis magnocellularis cholinergic system: one hundred years of progress. Neurobiol Learn Mem 1997;67:85–95. [PubMed: 9075237]

West MJ. New stereological methods for counting neurons. Neurobiol Aging 1993;14:275–285. [PubMed: 8367009]

Zaborszky L, Carlsen J, Brashear HR, Heimer L. Cholinergic and GABAergic afferents to the olfactory bulb in the rat with special emphasis on the projection neurons in the nucleus of the horizontal limb of the diagonal band. J Comp Neurol 1986;243:488–509. [PubMed: 3512629]

Abbreviations

A
amygdala

ac
anterior commissure

Acb
accumbens nucleus

ACh
acetylcholine

AD
anterodorsal thalamic nucleus

AHA
anterior hypothalamic area

AM
anteromedial thalamic nucleus

Arc
arcuate hypothalamic nucleus

AV
anteroventral thalamic nucleus

BF
basal forebrain

BST
bed nucleus of the stria terminalis

ChAT
choline acetyltransferase

Cl
claustrum

CM
central medial thalamic nucleus

CPu
caudate putamen

DBB
diagonal band of Broca nucleus

En
endopiriform nucleus

EP
entopeduncular nucleus

f
fornix

FStr
fundus striati

G
gelatinosus thalamic nucleus

GAD
glutamic acid decarboxylase

Glu
glutamate

GP
globus pallidus

IAM
interanteromedial thalamic nucleus

ic
internal capsule

LD
laterodorsal thalamic nucleus

LH
lateral hypothalamic area

lo
lateral olfactory tract

LOT
nucleus of the lateral olfactory tract

LPO
lateral preoptic area

LS
lateral septal nucleus

MCPO
magnocellular preoptic nucleus

MD
mediodorsal thalamic nucleus

MPO
medial preoptic nucleus

MS
medial septal nucleus

NR
neutral red

oc
optic chiasm

ot optic tract

OTu olfactory tubercle

Pa paraventricular hypothalamic nucleus

PAG phosphate-activated glutaminase

PC paracentral thalamic nucleus

Pe periventricular hypothalamic nucleus

Pir piriform cortex

PT paratenial thalamic nucleus

PV paraventricular thalamic nucleus

Re reuniens thalamic nucleus

Rh rhomboid thalamic nucleus

Rt reticular thalamic nucleus

SCh suprachiasmatic nucleus

SFi septofimbrial nucleus

SI substantia innominata

SIa substantia innominata anterior

SIp substantia innominata posterior

sm stria medullaris of the thalamus

SO supraoptic nucleus

st stria terminalis

TT
: tenia tecta

VAChT
: vesicular acetylcholine transporter

VGAT
: vesicular GABA transporter

VGluT
: vesicular glutamate transporter

VL
: ventrolateral thalamic nucleus

VM
: ventromedial thalamic nucleus

VMH
: ventromedial hypothalamic nucleus

ZI
: zona incerta

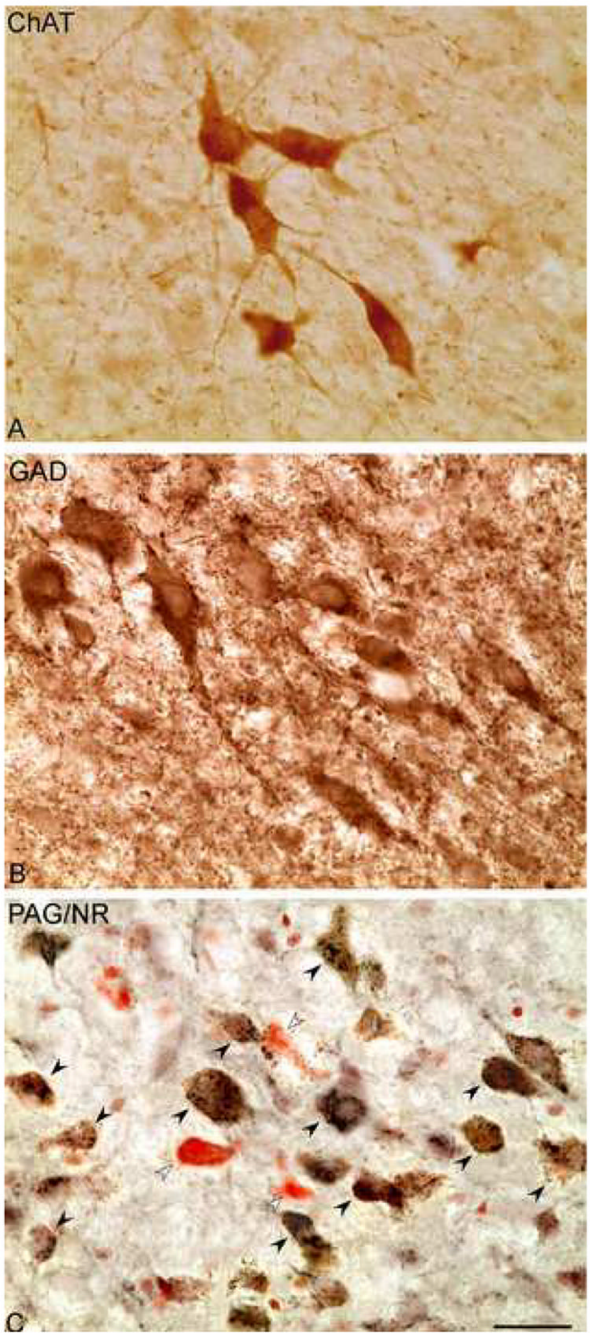

Fig. 1.

Images of ChAT+ (**A**), GAD+ (**B**) and PAG+ with NR+ (**C**) neurons in the magnocellular preoptic nucleus (MCPO, ~A8.5). ChAT and GAD are revealed with DAB (brown), and PAG is revealed with DAB-Ni (black) along with Nissl stained by Neutral Red (NR) (on right side in adjacent series from rat G3). Many cells are immuno-positive for PAG (PAG+/NR+, black arrowheads), evident as black granules over the cytoplasm, and are codistributed with fewer cells which are immuno-negative for PAG and stained for NR (PAG−/NR+, white arrowheads). Scale bar = 25 μm.

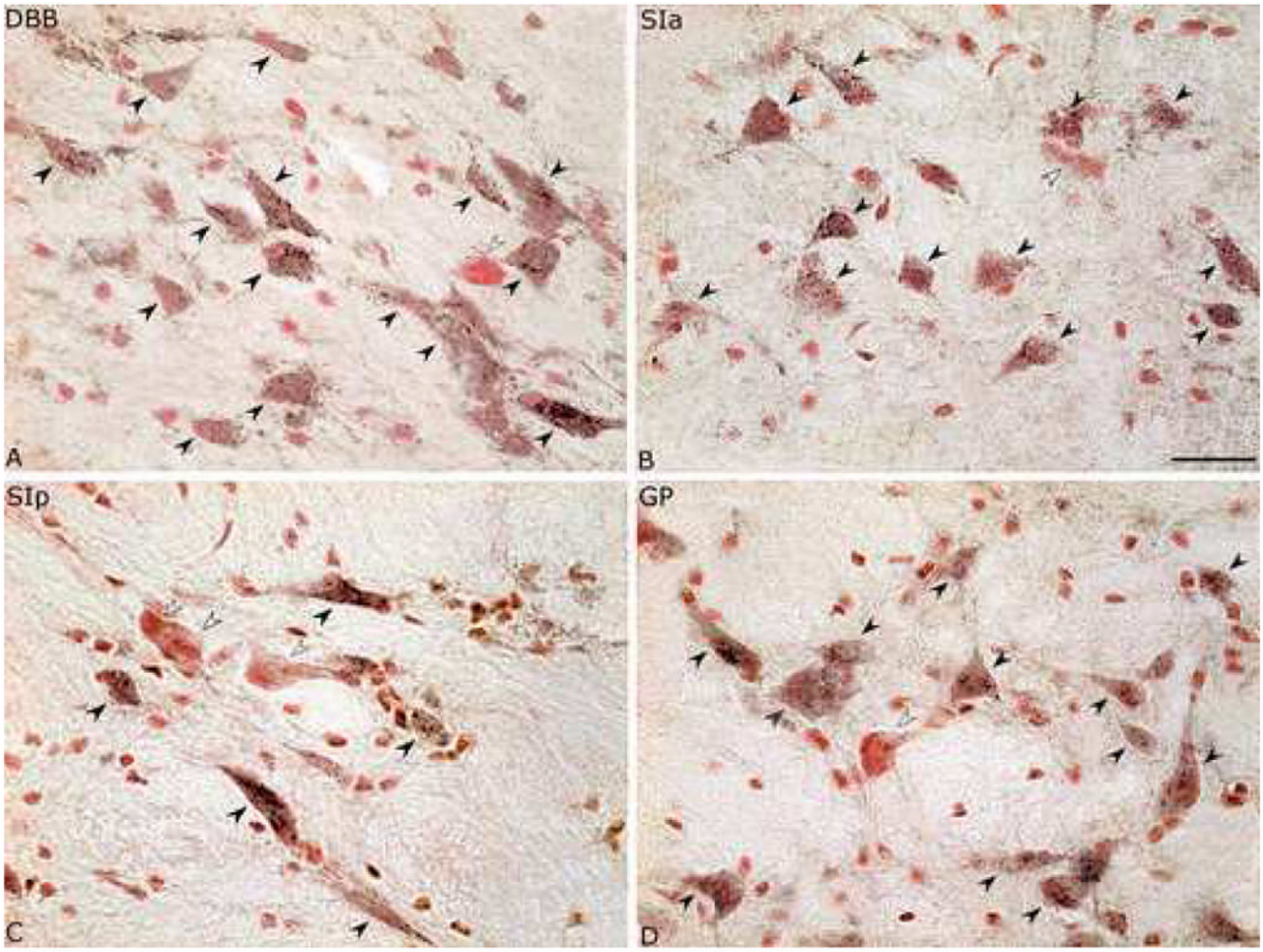

Fig. 2.

Images of PAG+/NR+ and PAG−/NR+ neurons in different BF nuclei. PAG+/NR+ cells (black arrowheads) are codistributed with PAG−/NR+ cells (white arrowheads) (on right side in same series from rat G3) in the nucleus of the diagonal band of Broca (DBB, ~A9.4, in **A**), the substantia innominata, pars anterior (SIa, ~A8.6 in **B**), the substantia innominata, pars posterior (SIp, A7.8 in **C**) and the globus pallidus (GP, ~A7.8 in **D**). Very small NR stained cells were judged to be glia and not counted as neurons. Scale bar = 25 μm.

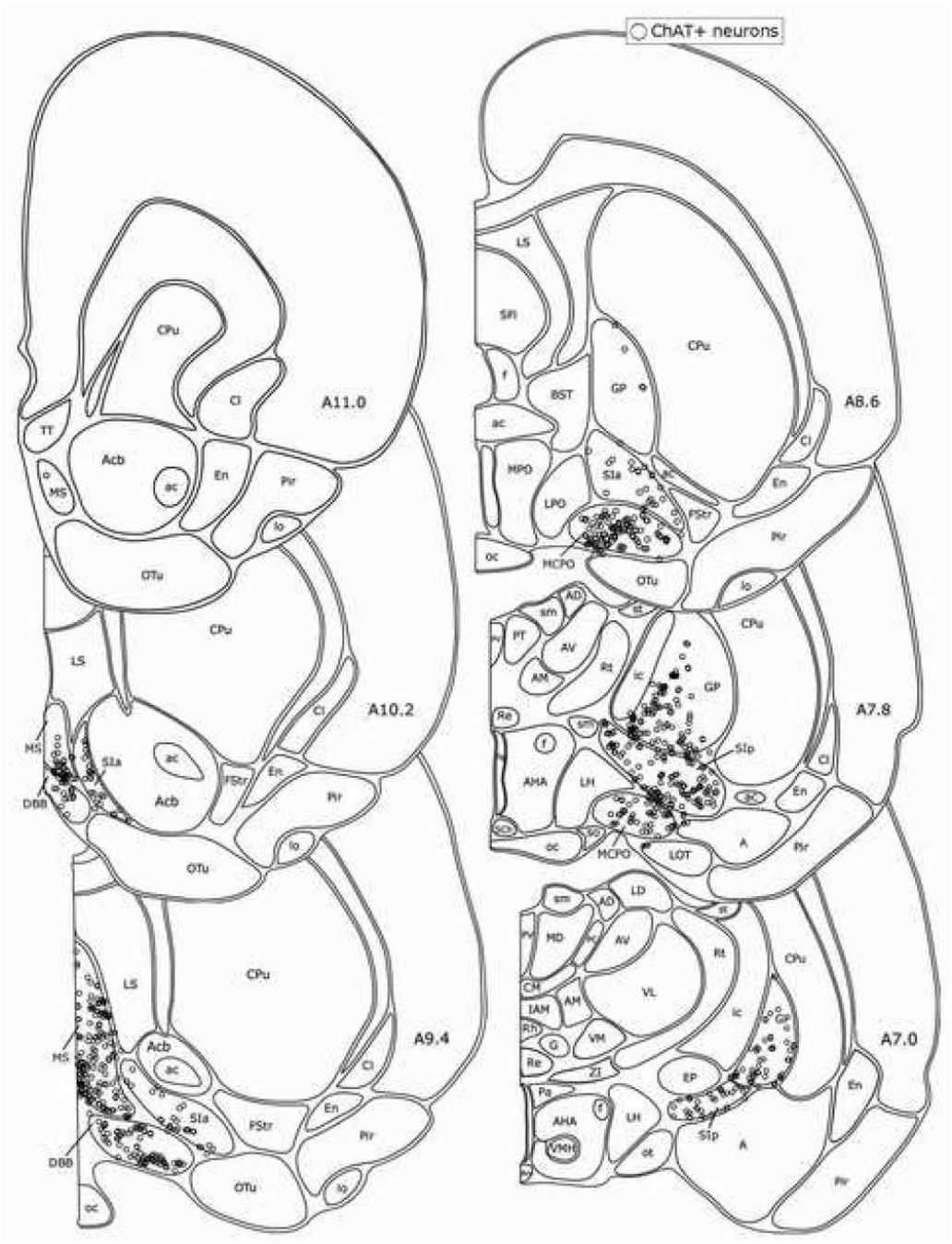

Fig. 3.

Distribution of ChAT+ neurons in the BF. Each symbol marks one ChAT+ cell plotted in one 20 μm thick section -based atlas templates. See (from list forrat G3) on abbreviations.

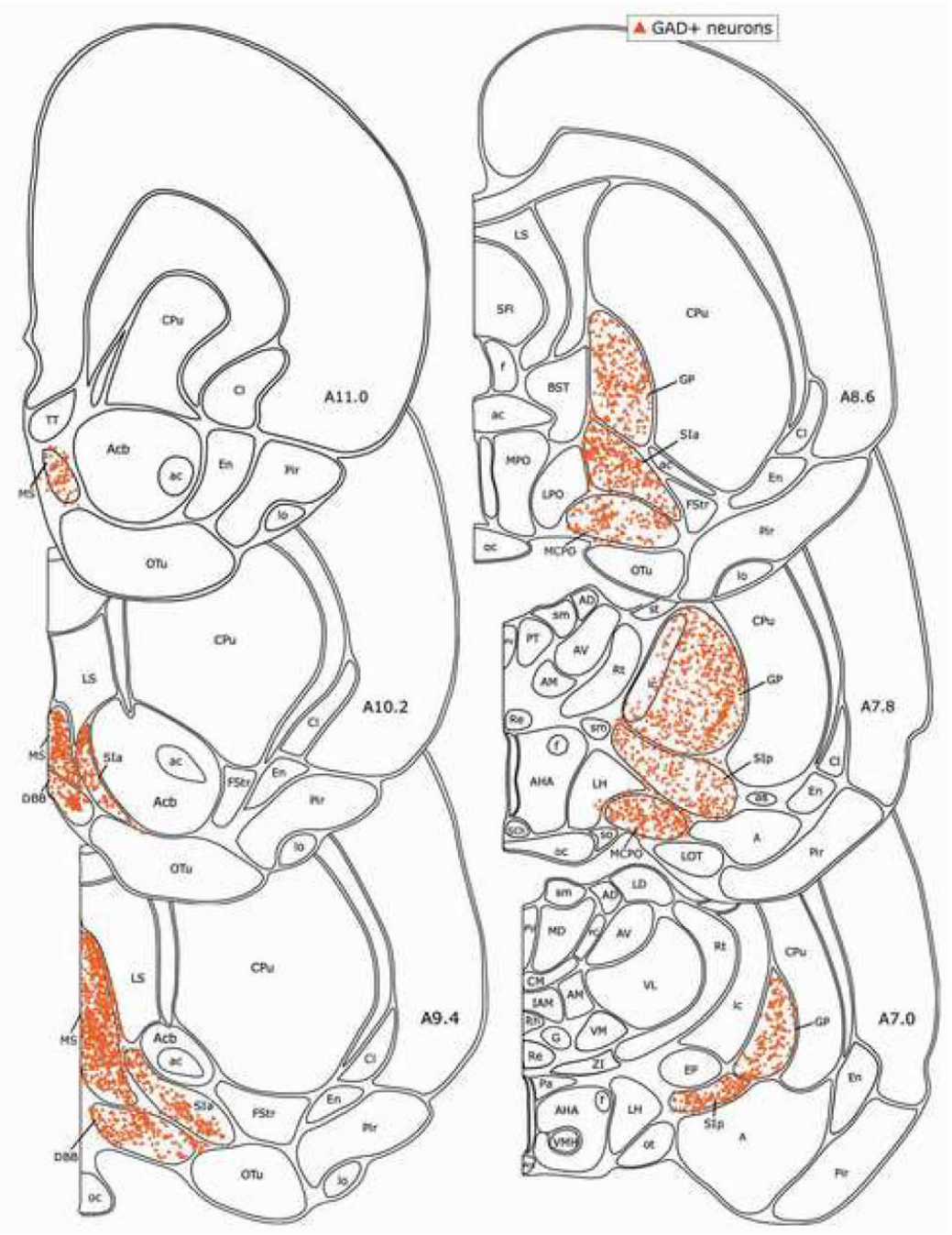

Fig. 4.

Distribution of GAD+ neurons in the BF. Each symbol marks one GAD+ cell plotted in one 20 μm thick section -based atlas templates. See list (from rat forG3) on abbreviations.

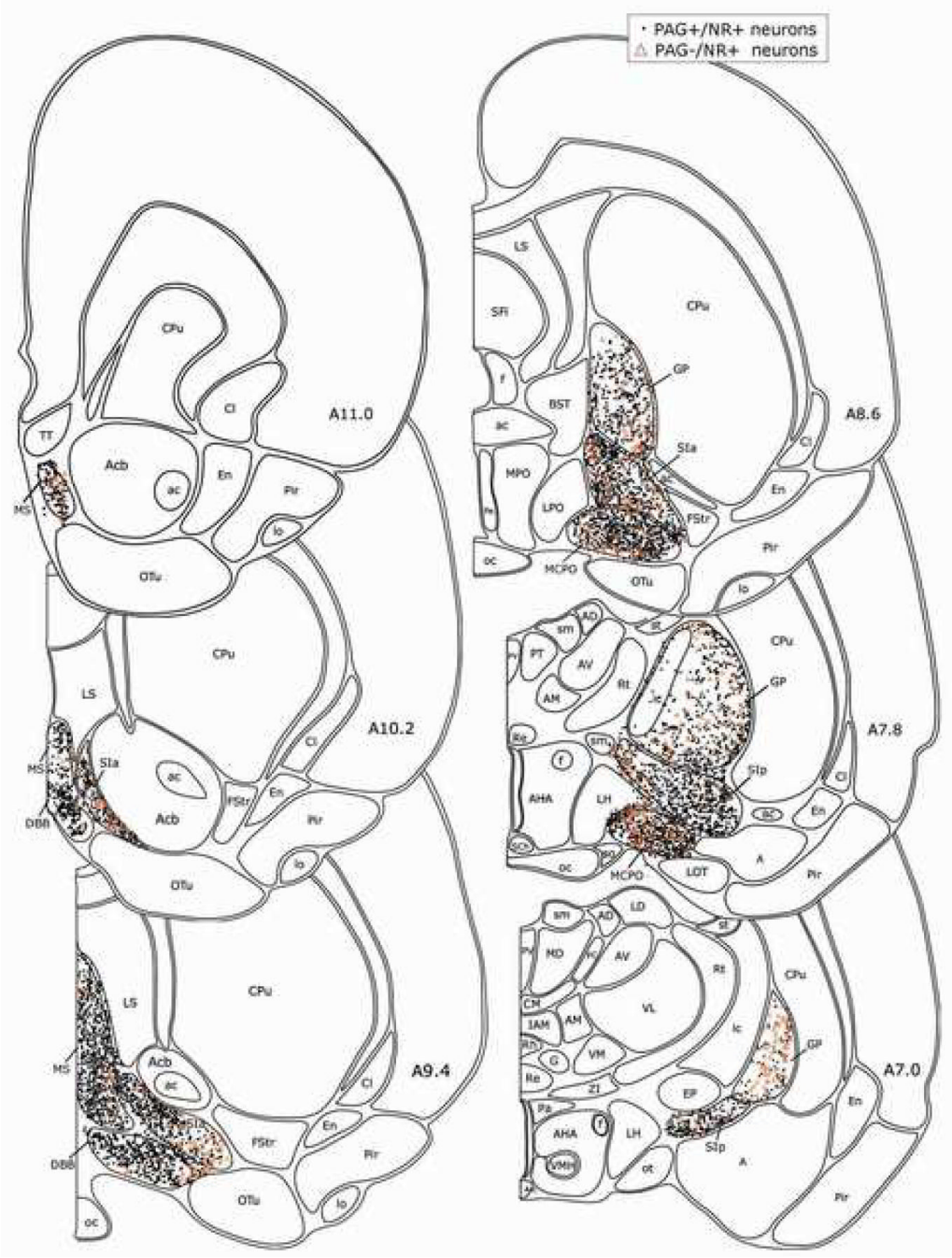

Fig. 5.

Distribution of PAG+/NR+ and PAG−/NR+ neurons in the BF. Each symbol marks one PAG +/NR+ or PAG−/NR+ cell plotted in one 20 μm-based atlas templates. See list for abbreviations.

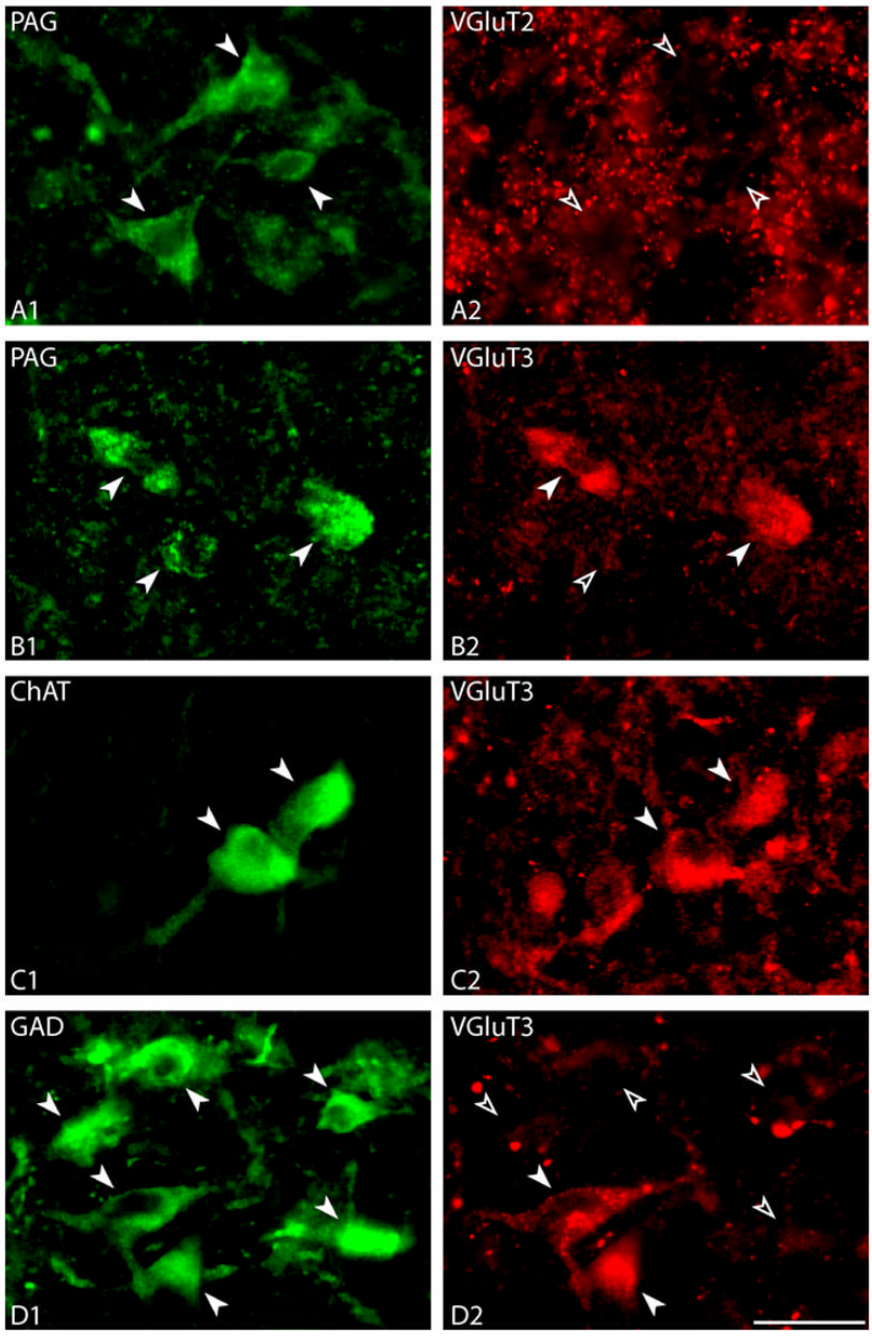

Fig. 6.

Presence of VGluT2 or VGluT3 in PAG+, ChAT+ or GAD+ cells in the MCPO of colchicine treated rats. **A**. PAG+ cells (in Cy2, solid arrowheads in **A1**) were not immunostained for VGluT2 (open arrowheads in **A2**), which was prominent in axonal terminals (in Cy3, **A2**). **B**. Most PAG+ cells (in Cy2, solid arrowheads in **B1**) were positively immunostained for VGluT3 (in Cy3, solid arrowheads in **B2**). **C**. Most ChAT+ cells (in Cy2, solid arrowheads in **C1**) were immunostained for VGluT3 (in Cy3, solid arrowhead in **C2**). **D**. About half of GAD + cells (in Cy2, solid arrowheads in **D1**) were judged immuno-positive (solid arrowheads in **D2**) and half immuno-negative (open arrowheads in **D2**) for VGluT3 immunostaining (in Cy3, **D2**). Scale bar = 25 μm.

Table 1

Stereological estimates of numbers and proportions of ChAT+, GAD+, PAG+ and total (NR+) cells in basal forebrain.

Sections Sampled Nucleus		Sites Sampled Mean ± SD	Volume (mm3) Mean ± SD	Cells Counted Mean ± SD	Cell Number Mean ± SD	Cell Density Mean ± SD	% Total Mean ± SD
ChAT+ cells							
MS	5	78.7 ± 1.5	0.939 ± 0.044	16.3 ± 15.0	2,062 ± 1,891	2,158 ± 1,954	4.4 ± 3.7
DBB	4	64.0 ± 5.3	0.738 ± 0.109	45.7 ± 13.2	5,765 ± 1,667	7,740 ± 1,379	14.5 ± 4.2
MCPO	5	104.7 ± 8.1	1.310 ± 0.112	43.0 ± 21.9	5,429 ± 2,769	4,147 ± 2,122	8.5 ± 4.3
SIa	7	187.0 ± 19.7	2.241 ± 0.245	17.0 ± 1.7	2,146 ± 219	969 ± 180	2.2 ± 0.2
SIp	4	100.0 ± 7.9	1.200 ± 0.094	21.7 ± 13.8	2,735 ± 1,742	2,275 ± 1,484	6.3 ± 3.4
GP	6	359.3 ± 10.2	4.941 ± 0.140	33.7 ± 13.7	4,250 ± 1,723	866 ± 364	6.1 ± 1.9
Total BF	**12**	**893.7 ± 23.0**	**11.369 ± 0.316**	**177.3 ± 57.7**	**22,388 ± 7,290**	**1,976 ± 661**	**6.2 ± 1.3**
GAD+ cells							
MS	5	79.7 ± 4.0	0.940 ± 0.046	120.7 ± 78.8	15,234 ± 9,946	16,279 ± 10,473	36.9 ± 24.1
DBB	4	66.0 ± 8.7	0.765 ± 0.136	62.7 ± 34.4	7,911 ± 4,347	9,891 ± 4,581	20.6 ± 12.4
MCPO	5	106.3 ± 7.5	1.313 ± 0.092	131.0 ± 78.1	16,538 ± 9,860	12,806 ± 8,074	26.2 ± 15.6
SIa	7	181.7 ± 12.5	2.173 ± 0.197	216.0 ± 130.0	27,269 ± 16,411	12,652 ± 8,138	29.2 ± 17.9
SIp	4	101.3 ± 4.7	1.210 ± 0.087	63.0 ± 26.5	7,954 ± 3,347	6,508 ± 2,429	20.6 ± 10.1
GP	6	358.7 ± 10.5	4.932 ± 0.135	353.0 ± 47.5	44,565 ± 5,992	9,052 ± 1,351	65.7 ± 6.8
Total BF	**12**	**893.7 ± 13.6**	**11.334 ± 0.276**	**946.3 ± 369.6**	**119,471 ± 46,657**	**10,528 ± 4,107**	**34.1 ± 12.8**
PAG+ cells							
MS	5	78.3 ± 2.3	0.939 ± 0.044	309.0 ± 56.6	39,010 ± 7,149	41,384 ± 5,832	90.5 ± 5.7
DBB	4	62.0 ± 7.8	0.738 ± 0.109	287.0 ± 64.0	36,233 ± 8,080	49,811 ± 12,461	89.6 ± 5.8
MCPO	5	103.7 ± 6.0	1.328 ± 0.088	470.0 ± 60.5	59,336 ± 7,639	44,571 ± 3,007	92.7 ± 2.0
SIa	7	185.0 ± 12.2	2.193 ± 0.163	653.3 ± 54.2	82,481 ± 6,848	37,881 ± 5,594	85.6 ± 7.8
SIp	4	100.7 ± 7.2	1.197 ± 0.096	292.0 ± 64.0	36,864 ± 8,083	30,979 ± 7,744	90.0 ± 0.7
GP	6	356.3 ± 4.7	4.910 ± 0.069	494.7 ± 115.9	62,450 ± 14,632	12,713 ± 2,920	90.8 ± 2.3
Total BF	**12**	**886.3 ± 15.0**	**11.304 ± 0.235**	**2,506.0 ± 347.4**	**316,374 ± 43,860**	**28,006 ± 3,992**	**89.4 ± 3.7**
NR+ cells (Total)							
MS	5	78.3 ± 2.3	0.939 ± 0.044	342.3 ± 65.3	43,218 ± 8,245	45,832 ± 6,829	100.0 ± 0.0
DBB	4	62.0 ± 7.8	0.738 ± 0.109	321.7 ± 74.5	40,609 ± 9,411	56,222 ± 16,845	100.0 ± 0.0
MCPO	5	103.7 ± 6.0	1.328 ± 0.088	508.0 ± 76.5	64,133 ± 9,663	48,129 ± 4,243	100.0 ± 0.0
SIa	7	185.0 ± 12.2	2.193 ± 0.163	769.7 ± 115.6	97,168 ± 14,591	44,777 ± 9,677	100.0 ± 0.0
SIp	4	100.7 ± 7.2	1.197 ± 0.096	324.7 ± 73.0	40,988 ± 9,216	34,438 ± 8,759	100.0 ± 0.0
GP	6	356.3 ± 4.7	4.910 ± 0.069	544.7 ± 124.1	68,762 ± 15,672	13,995 ± 3,113	100.0 ± 0.0
Total BF	**12**	**886.3 ± 15.0**	**11.304 ± 0.235**	**2,811.0 ± 432.2**	**354,879 ± 54,558**	**31,433 ± 5,132**	**100.0 ± 0.0**

Cells were counted and total cell numbers estimated using the Optical Fractionator prob0e of StereoInvestigator in the number of sections (every 400 μm) and sites (89 x 89 μmby 8 μm depth counting blocks) indicated along with the estimated volume and corresponding cell density (per mm^3) per nucleus. The % total represents the proportion that each cell type represents of the Nissl-stained (NR +) cells per nucleus, which was calculated as the total number of NR+ (PAG+/NR+ plus PAG−/NR+) cells.